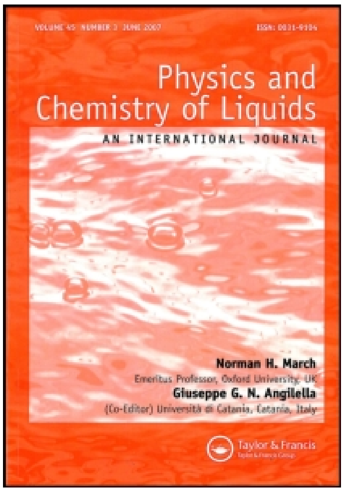

Physics and Chemistry of Liquids
Publication details, including instructions for authors and subscription information:
http://www.informaworld.com/smpp/title~content=t713646857

Ultrasonic velocities, isentropic compressibilities and excess molar volumes of octan-1-ol with chloroform, 1,2-dichloroethane and 1,1,2,2-tetrachloroethane at 298.15 and 308.15 K

Subhash C. Bhatia[a]; Rachna Bhatia[a]; Gyan P. Dubey[a]
[a] Department of Chemistry, Kurukshetra University, Kurukshetra 136119, India

To cite this Article Bhatia, Subhash C. , Bhatia, Rachna and Dubey, Gyan P.(2010) 'Ultrasonic velocities, isentropic compressibilities and excess molar volumes of octan-1-ol with chloroform, 1,2-dichloroethane and 1,1,2,2-tetrachloroethane at 298.15 and 308.15 K', Physics and Chemistry of Liquids, 48: 2, 199 — 230

To link to this Article: DOI: 10.1080/00319100902774516

URL: http://dx.doi.org/10.1080/00319100902774516

Physics and Chemistry of Liquids
Vol. 48, No. 2, April 2010, 199–230

Ultrasonic velocities, isentropic compressibilities and excess molar volumes of octan-1-ol with chloroform, 1,2-dichloroethane and 1,1,2,2-tetrachloroethane at 298.15 and 308.15 K

Subhash C. Bhatia*, Rachna Bhatia and Gyan P. Dubey

Department of Chemistry, Kurukshetra University, Kurukshetra 136119, India

(*Received 16 November 2007; final version received 25 January 2009*)

Densities (ρ), and ultrasonic velocities (u) of binary mixtures of octan-1-ol with chloroform, 1,2-dichloroethane, and 1,1,2,2-tetrachloroethane (TCE) have been measured over the entire range of composition at 298.15 and 308.15 K and at atmospheric pressure. From the experimental values of density and ultrasonic velocity, the excess molar volumes (V^{E}), deviations in ultrasonic velocity (Δu), intermolecular free lengths (L_{f}), mean molecular radii (r), molar sound velocities (R_m), acoustic impedances (Z), excess isentropic compressibilities (κ_s^{E}), excess intermolecular free lengths ($L_{\mathrm{f}}^{\mathrm{E}}$) and excess acoustic impedances (Z^{E}) have been calculated. These excess functions have been fitted to the Redlich–Kister polynomial equation to derive the binary coefficients and the standard errors between the experimental and the calculated quantities. The experimental ultrasonic velocities have been analysed in terms of Nomoto (N), Van Dael (VD), Jacobson's free length theory, Schaaffs collision factor theory and thermoacoustical parameters.

Keywords: octan-1-ol + haloalkanes; isentropic compressibility; free intermolecular length; acoustic impedance

1. Introduction

The mixing of different liquids produces solutions that generally do not behave ideally. The deviation from the ideal behaviour can be expressed by many thermodynamic variables, particularly by excess properties. The excess thermodynamic properties of liquid mixtures relate to the difference between the actual property and the property if the system behaves ideally. These properties are quite useful in the study of the nature of molecular interactions in the liquid mixtures. In particular, they correspond to the interactions that take place between solute–solute (A–A), solvent–solvent (B–B) and solute–solvent (A–B) species. The mixture thermodynamic properties obtained from a measurement of density and velocity of sound can provide an insight into the nature of molecular interactions in liquid mixtures. A literature survey indicates that not much work has been carried out on the study of thermodynamic properties of binary mixtures of haloalkanes with

---

*Corresponding author. Email: bhatiasc2@rediffmail.com

ISSN 0031–9104 print/ISSN 1029–0451 online

DOI: 10.1080/00319100902774516
http://www.informaworld.com

higher alkanols. The variations in the volumetric and acoustic properties of the binary mixtures of alkanols containing haloalkanes, acetonitrile, ethylacetate and ethenyl ethanoate, with the molecular size, shape, chain-length and degree of molecular association of normal alkanols and branched alkanols have been reported earlier [1–12]. Alkanols are polar and self-associated liquids and the dipolar association of alkanols decreases when they are mixed with polar compounds containing halogen atoms, due to some sort of specific intermolecular interactions between the hydroxyl oxygen of alkanols and the haloalkanes [8–13]. Here, we report the experimental results of density (ρ) and ultrasonic velocity (u) of binary liquid mixtures of octan-1-ol with chloroform, 1,2-dichloroethane (DCE) and 1,1,2,2-tetrachloroethane (TCE) at 298.15 and 308.15 K over the entire range of mixture mole fraction. From the experimental values of density (ρ) and ultrasonic velocity (u), the excess molar volumes (V^{E}), deviations in velocity of sound (Δu), isentropic compressibilities (κ_S), intermolecular free lengths (L_f), mean molecular radii (r), molar sound velocities (R_m), acoustic impedances (Z), excess isentropic compressibilities (κ_s^E), excess intermolecular free lengths (L_f^E) and excess acoustic impedances (Z^E) have been calculated. These quantities have been fitted to the Redlich–Kister [14] polynomial equation to derive the binary coefficients (A_i) and standard errors (σ) between the experimental and the calculated quantities.

2. Experimental section

2.1. *Materials*

The mole fraction purity of the liquids from S.D. fine Chemical Ltd. were as follows: Chloroform (99.7%) 1,2-DCE (99.5%), 1,1,2,2-TCE (99.4%) and octan-1-ol (99.7%). Density and ultrasonic velocity values of the pure liquids and their mixtures at 298.15 and 308.15 K were measured with Anton Paar digital densimeter (model DSA 5000) operated in the static mode and automatically thermostated within ±0.001 K.

The densities have precision better than $\pm 10^{-3}\,\mathrm{kg\,m^{-3}}$ and the velocity of sound values are accurate to $\pm 0.01\,\mathrm{m\,s^{-1}}$. Densities and ultrasonic velocities of the pure liquids were in good agreement with the values found in the literature [15–20] (Table 1).

2.2. *Apparatus and procedure*

Before each series measurements, the instrument was calibrated with double-distilled freshly degassed water and dry air at atmospheric pressure. Densities of both water and dry air at the various working temperatures were supplied by the manufacturer in the instruction manual. The calibration was accepted if the measurements were within $2 \times 10^{-6}\,\mathrm{g\,cm^{-3}}$ of the published values. The uncertainties were estimated to be within $\pm 2 \times 10^{-6}\,\mathrm{g\,cm^{-3}}$. Air-tight stoppered bottles were used for the preparation of mixtures. The mass of the dry bottle was first determined. The less volatile component of the mixture was introduced in the bottle, and the total mass was measured. Subsequently, the other liquid component was introduced, and the mass of bottle along with the two components were determined. All the mixtures were weighed on an electronic balance accurate to 0.1 mg. The average uncertainty in the

Table 1. Physical properties of pure liquid components.

		ρ (g cm^{-3})		u (m s^{-1})		α (kK)$^{-1}$	
Pure liquid	Temperature (K)	Expt	Lit	Expt	Lit	Expt	Lit
Octan-1-ol	298.15	0.821821	0.821826[a] 0.821620[b]	1348.34	1347.50[e] 1347.32[b]	0.8591	0.827[g]
Chloroform	298.15	1.472435	1.4788[c]	983.58	967 (at 303.15 K)[f]	1.3085	1.30 (303.15 K)[f]
1,2 Dichloroethane	298.15	1.24529	1.24564[d]	1194.06	–	1.1933	1.169[d]
1,1,2,2,-Tetrachloroethane	298.15	1.588539	1.58683[d]	1071.68	–	0.9942	0.979[d]

Notes: [a][15], [b][16], [c][17], [d][1], [e][18], [f][19], [g][20].

mole fraction of the mixtures was estimated to be less than $\pm 2 \times 10^{-4}$. From the results of velocity of sound, the isentropic compressibility, κ_S, was calculated using the Laplace relation [4]

$$\kappa_s = \frac{1}{u^2 \rho}. \tag{1}$$

The results of ρ and u compiled in Table 2 represent the average of at least three independent measurements for each composition of the mixture.

3. Results and discussion

The excess molar volumes of the solutions were calculated from the densities of the pure liquids and their mixtures using the following equation:

$$V^{\mathrm{E}}(\mathrm{cm}^3 \cdot \mathrm{mol}^{-1}) = (x_1 M_1 + x_2 M_2)/\rho_{\mathrm{mix}} - (x_1 M_1/\rho_1 + x_2 M_2/\rho_2), \tag{2}$$

where ρ_{mix} is the density of the mixture and x_1, M_1, ρ_1 and x_2, M_2 and ρ_2 are the mole fraction, molecular weight and the density of pure components 1 and 2, respectively. The excess molar volumes were reproducible to $\pm 2 \times 10^{-3}\,\mathrm{cm}^3\,\mathrm{mol}^{-1}$. The first term in Equation (2) represents the actual volume of the mixture, V_{mix} and the second, the volume it would occupy if the mixture behaved ideally, V_{id}.

The following relations have been used to calculate the sound velocity (u) of the binary liquid mixtures:

Nomoto Relation [21]

$$u = \left(\frac{R_{\mathrm{m}}}{V_{\mathrm{mix}}}\right)^3 = \left(\frac{x_1 R_1 + x_2 R_2}{x_1 v_1 + x_2 v_2}\right)^3, \tag{3}$$

where x_1, x_2; v_1, v_2 and R_1, R_2 are mole fractions; molar volumes and molar sound velocity of first and second components, respectively. The molar sound velocity (R_{m}) is given by the relation

$$R_{\mathrm{m}} = (M/\rho) u^{1/3}. \tag{4}$$

Van Dael relation [22]

$$\frac{1}{x_1 M_1 + x_2 M_2} \cdot \frac{1}{u^2_{\mathrm{id,\,mix}}} = \frac{x_1}{M_1 u_1^2} + \frac{x_2}{M_2 u_2^2}, \tag{5}$$

where M_1, M_2 and u_1, u_2 are the molecular weights and sound velocities of first and second components, respectively, and $u_{\mathrm{id,mix}}$ is the ultrasonic velocity of the ideal mixture.

Jacobson's free length theory (FLT) [23]

$$u_{\mathrm{mix}} = \frac{K}{L_{\mathrm{f(mix)}} \rho_{\mathrm{mix}}^{1/2}}, \tag{6}$$

where K is the Jacobson constant which is temperature dependent only and its values at 298.15 and 308.15 K are 623.34 and 633.71, respectively, $L_{\mathrm{f(mix)}}$ is the

Table 2. Density ρ, ultrasonic velocity u, isentropic compressibility κ_s, excess molar volume V^E, excess isentropic compressibility κ_s^E for haloalkanes + octan-1-ol (2) at (298.15 and 308.15) K.

x_1	ϕ_1	$\rho \times 10^{-3}$ (kg m^{-3})	u (m s^{-1})	$\kappa_s \times 10^{12}$ (Pa^{-1})	$V^E \times 10^6$ (m^3 mol^{-1})	$\kappa_s^E \times 10^{12}$ (Pa^{-1})	ϕ_1	$\rho \times 10^{-3}$ (kg m^{-3})	u (m s^{-1})	$\kappa_s \times 10^{12}$ (Pa^{-1})	$V^E \times 10^6$ (m^3 mol^{-1})	$\kappa_s^E \times 10^{12}$ (Pa^{-1})
Chloroform (1) + Octan-1-ol (2) (298.15 K)							Chloroform (1) + Octan-1-ol (2) (308.15 K)					
0.0000	0.0000	0.821821	1348.29	669.35	0.000	0.00	0.0000	0.814835	1314.45	710.30	0.000	0.00
0.0351	0.0183	0.833605	1336.53	671.56	0.022	−0.04	0.0184	0.826219	1302.96	712.92	0.066	−0.11
0.1707	0.0953	0.882361	1290.65	680.36	0.237	−0.19	0.0957	0.874139	1256.00	725.17	0.297	1.18
0.2493	0.1452	0.913941	1262.42	686.55	0.362	0.66	0.1458	0.905311	1227.78	732.76	0.407	2.16
0.2913	0.1737	0.931900	1246.90	690.19	0.430	1.41	0.1744	0.922880	1212.46	737.09	0.490	2.90
0.3610	0.2243	0.963882	1220.18	696.83	0.520	3.27	0.2250	0.954459	1186.27	744.52	0.561	4.32
0.3986	0.2532	0.982341	1205.49	700.50	0.549	4.38	0.2541	0.972641	1172.07	748.41	0.585	4.96
0.5134	0.3505	1.044551	1160.33	711.06	0.606	7.38	0.3516	1.033698	1127.14	761.47	0.650	8.22
0.6148	0.4495	1.108202	1119.27	720.30	0.608	10.70	0.4506	1.096240	1086.71	772.44	0.646	11.14
0.6369	0.4729	1.123323	1110.30	722.13	0.603	11.40	0.4741	1.111080	1077.32	775.47	0.640	12.56
0.6616	0.5000	1.140813	1100.31	724.03	0.596	12.14	0.5012	1.128264	1067.11	778.34	0.630	13.71
0.7463	0.6008	1.206223	1066.55	728.80	0.543	13.95	0.6019	1.192762	1033.75	784.54	0.546	14.99
0.8015	0.6739	1.253879	1045.09	730.19	0.490	14.61	0.6749	1.239921	1012.85	786.17	0.457	14.58
0.9017	0.8243	1.353477	1009.80	724.57	0.304	11.65	0.8249	1.336879	977.25	783.24	0.314	11.90
0.9822	0.9658	1.448509	987.94	707.32	0.096	2.67	0.9660	1.429928	953.61	769.03	0.098	4.06
1.0000	1.0000	1.472435	983.80	701.70	0.000	0.00	1.0000	1.453331	949.98	762.44	0.000	0.00
1,2-Dichloroethane (1) + Octan-1-ol (2) (298.15 K)							1,2-Dichloroethane (1) + Octan-1-ol (2) (308.15 K)					
0.0000	0.0000	0.821821	1348.29	669.35	0.000	0.00	0.0000	0.814835	1314.45	710.30	0.000	0.00
0.0492	0.0253	0.831980	1338.36	671.03	0.103	3.34	0.0254	0.824777	1304.55	712.43	0.115	3.49
0.0906	0.0476	0.841125	1328.66	673.46	0.152	7.28	0.0477	0.833611	1294.70	715.65	0.196	7.95
0.2242	0.1266	0.872960	1301.89	675.86	0.397	15.29	0.1270	0.864628	1267.67	719.71	0.490	16.76
0.3387	0.2044	0.904188	1277.56	677.61	0.608	23.02	0.2049	0.895061	1243.02	723.09	0.737	25.32
0.4467	0.2882	0.937500	1255.47	676.73	0.836	29.10	0.2889	0.927690	1220.75	723.34	0.971	31.77
0.4963	0.3307	0.954090	1245.89	675.23	0.972	31.34	0.3315	0.944121	1211.02	722.22	1.085	34.05
0.5965	0.4257	0.991000	1228.15	669.00	1.248	34.00	0.4266	0.981119	1192.00	717.34	1.266	37.40
0.6663	0.5003	1.021011	1216.10	662.26	1.315	34.80	0.5012	1.010682	1179.94	710.67	1.323	37.83

(*continued*)

Table 2. Continued.

x_1	ϕ_1	$\rho \times 10^{-3}$ (kg m^{-3})	u (m s^{-1})	$\kappa_s \times 10^{12}$ (Pa^{-1})	$V^E \times 10^6$ (m^3 mol^{-1})	$\kappa_s^E \times 10^{12}$ (Pa^{-1})	ϕ_1	$\rho \times 10^{-3}$ (kg m^{-3})	u (m s^{-1})	$\kappa_s \times 10^{12}$ (Pa^{-1})	$V^E \times 10^6$ (m^3 mol^{-1})	$\kappa_s^E \times 10^{12}$ (Pa^{-1})
0.7304	0.5760	1.051951	1206.47	653.09	1.322	33.76	0.5768	1.041145	1171.12	700.30	1.321	35.29
0.7590	0.6123	1.067371	1202.08	648.36	1.268	33.13	0.6131	1.055994	1166.78	695.60	1.294	34.56
0.9085	0.8328	1.166695	1189.44	605.84	0.578	18.23	0.8332	1.152910	1154.10	651.20	0.633	17.74
0.9535	0.9114	1.202863	1191.69	585.41	0.338	8.87	0.9116	1.188599	1154.90	630.78	0.370	8.67
0.9616	0.9262	1.211276	1192.66	580.39	0.189	6.04	0.9265	1.196659	1155.40	625.99	0.233	6.13
0.9896	0.9795	1.235880	1193.92	567.64	0.047	1.27	0.9795	1.221362	1155.87	612.83	0.046	1.27
1.0000	1.0000	1.245290	1194.06	563.22	0.000	0.00	1.0000	1.230566	1155.85	608.26	0.000	0.00
		1,1,2,2-Tetrachloroethane(1) + Octan-1-ol (2) (298.15 K)						1,1,2,2-Tetrachloroethane(1) + Octan-1-ol (2) (308.15 K)				
0.0000	0.0000	0.821821	1348.29	669.35	0.000	0.00	0.0000	0.814835	1314.45	710.30	0.000	0.00
0.0391	0.0264	0.842247	1337.38	663.82	−0.033	−0.88	0.0264	0.835020	1303.85	704.45	−0.027	−1.01
0.0672	0.0459	0.857205	1329.69	659.80	−0.041	−1.45	0.0459	0.849791	1296.23	700.36	−0.027	−1.50
0.1413	0.0989	0.897712	1309.54	649.57	−0.017	−2.25	0.0990	0.889839	1276.25	689.95	0.004	−2.09
0.2172	0.1561	0.941184	1288.88	639.59	0.050	−1.95	0.1563	0.932822	1255.81	679.76	0.077	−1.58
0.2704	0.1982	0.973175	1274.92	632.18	0.087	−1.73	0.1984	0.964465	1242.04	672.11	0.115	−1.28
0.4038	0.3111	1.059013	1241.29	612.85	0.170	−0.35	0.3114	1.049326	1208.96	652.03	0.203	0.23
0.4464	0.3496	1.088334	1231.12	606.23	0.193	0.21	0.3499	1.078380	1199.12	644.92	0.219	0.59
0.5512	0.4503	1.164800	1208.10	588.22	0.250	1.17	0.4506	1.154015	1176.25	626.31	0.273	1.76
0.6371	0.5393	1.232608	1190.86	572.08	0.277	2.10	0.5397	1.220952	1159.45	609.25	0.309	2.53
0.6830	0.5896	1.270907	1182.63	562.59	0.283	2.38	0.5899	1.258812	1151.35	599.27	0.314	2.74
0.7481	0.6644	1.328105	1172.37	547.82	0.283	2.37	0.6647	1.315351	1141.27	583.69	0.311	2.56
0.8561	0.7987	1.431405	1158.78	520.28	0.220	1.86	0.7989	1.417371	1127.84	554.65	0.248	1.76
0.9321	0.9015	1.510941	1153.22	497.65	0.151	0.49	0.9016	1.496361	1121.96	530.90	0.145	0.23
0.9834	0.9753	1.568971	1150.51	481.51	0.041	−0.09	0.9753	1.553566	1118.71	514.32	0.042	−0.06
1.0000	1.0000	1.588539	1149.63	476.31	0.000	0.00	1.0000	1.572901	1117.78	508.85	0.000	0.00

intermolecular free length of the binary mixture and ρ_{mix} is the density of the mixture.

$$L_{\mathrm{f}} = \frac{2V_{\mathrm{a}}}{Y}: \tag{7}$$

where V_{a} represents the available volume per mole and Y is the surface area per mole and can be expressed as

$$V_a = V_T - V_0, \tag{8}$$

$$Y = \left(36\pi N V_0^2\right)^{1/3}. \tag{9}$$

Here, N is the Avogadro number and V_0 and V_T are the molar volumes at zero Kelvin and at temperature T, respectively. V_0 can be obtained from the following relation using critical temperature T_{c}:

$$V_0 = V_T(1 - T/T_{\mathrm{c}})^{0.3}. \tag{10}$$

In the present work, the critical temperature of the systems under consideration is supposed to be the mole fraction additive of the values of its pure components and is given by the relation:

$$T_{\mathrm{c}} = x_1 T_{\mathrm{c}(1)} + x_2 T_{\mathrm{c}(2)}. \tag{11}$$

Assuming additivity of the surface area, the thermodynamic intermolecular free lengths in the binary liquid mixtures have been calculated using the relation:

$$L_f = \frac{2\left[V_T - \left\{x_1 V_{0(1)} + x_2 V_{0(2)}\right\}\right]}{x_1 Y_1 + x_2 Y_2}. \tag{12}$$

The intermolecular free lengths (L_{f}) have also been computed using Equations (7) and (9) and the Schaaff's relation for available volume (V_{a}):

$$V_{\mathrm{a}} = V_T\left[1 - \left(\frac{u}{u_\infty}\right)\right], \tag{13}$$

where u is the ultrasonic velocity at temperature T and u_∞ is $1600\,\mathrm{m\,s^{-1}}$. The L_{f} obtained by this approach is known as ultrasonic intermolecular free length.

Schaaffs collision factor theory (CFT) [24–26]

$$u_{\mathrm{mix}} = u_\infty(x_1 S_1 + x_2 S_2)\frac{[(x_1 b_1 + x_2 b_2)]}{V_{\mathrm{mix}}}, \tag{14}$$

where b and S are the geometric volume and collision factor, respectively. The actual volume of the molecule per mole of the liquid has been computed using the relations

$$b = \frac{4}{3}\pi r^3 N, \tag{15}$$

where r is the molecular radius which has been computed using the relations

$$b' = \left[\frac{M}{\rho} - \frac{\gamma RT}{\rho u^2}\left(\left(1 + \frac{Mu^2}{3\gamma RT}\right)^{1/2} - 1\right)\right] \tag{16}$$

$$r = \left(\frac{3b'}{16\pi N}\right)^{1/3}, \tag{17}$$

where b' is the van der Waals constant and is equal to four times the actual volume of the molecules per mole of the liquid, i.e. $b' = 4b$, and γ is the ratio of the principle heat capacities, i.e. $\gamma = C_P/C_V$.

The value of the collision factor S has been calculated using the relation

$$S = \frac{uV_T}{bu_\infty}. \tag{18}$$

3.1. *Thermoacoustical approach*

Thermoacoustical method has also been employed to obtain the available volume using the relation [19]

$$V_a = V_T\left(\frac{1}{K' + 1}\right) = V_T\left(\frac{1}{K + K'' + 1}\right). \tag{19}$$

K', K and K'' are known as isothermal, isobaric and isochoric acoustical parameters and can be expressed by the relations:

$$K' = K + K'' = \frac{1}{2}\left[3 + \frac{S*(1 + \alpha T) + X}{\alpha T}\right] \tag{20}$$

$$K'' = 1 + X/2\alpha T$$

$$K = \frac{1}{2}\left[1 + \frac{S*(1 + \alpha T)}{\alpha T}\right] \tag{21}$$

$$S^* = 1 + \frac{4\alpha T}{3}. \tag{22}$$

X is known as the isochoric temperature coefficient of internal pressure and can be expressed as

$$X = 2\left(\frac{1 + 2\alpha T}{\overline{V}^{C_1}}\right), \tag{23}$$

where $\overline{V}$ represents the reduced molar volume and C_1 is the Moelwyn–Hughes parameter and can be expressed as

$$\overline{V} = \left[\frac{\alpha T/3}{1 + \alpha T} + 1\right]^3 \tag{24}$$

$$C_1 = \frac{13}{3} + \frac{1}{\alpha T} + \frac{4\alpha T}{3}. \tag{25}$$

The thermal expansion coefficients, α, have been calculated from the Equation [27]

$$\alpha = \frac{1}{\rho}\left(\frac{\partial \rho}{\partial T}\right)_P. \tag{26}$$

Acoustic impedance (Z) has been calculated using the relation [28]

$$Z = u_{\text{mix}}\rho_{\text{mix}}. \tag{27}$$

The values of Δu, L_{f}^{E}, and Z^{E} have been calculated using the general equation [28]

$$\Delta Y = Y_{\text{mix}} - (Y_1 x_1 + Y_2 x_2), \tag{28}$$

where ΔY is Δu or L_{f}^{E} or Z^{E}.

The excess isentropic compressibility (κ_s^{E}) was obtained using the relation [4,29,30]

$$\kappa_s^{\text{E}} = k_s - \kappa_s^{\text{id}}, \tag{29}$$

where the isentropic compressibility term k_s^{id} was computed using the relation

$$\kappa_s^{\text{id}} = \sum_{i=1}^{2}\phi_i\left[\kappa_{s,i} + \frac{TV_i\left(\alpha_i^2\right)}{C_{P,i}}\right] - \left\{\frac{T\left(\sum_{i=1}^{2} x_i V_i\right)\left(\sum_{i=1}^{2}\phi_i\alpha_i\right)^2}{\sum_{i=1}^{2} x_i C_{P,i}}\right\}. \tag{30}$$

Here, $C_{P,i}$ is the molar heat capacity of the i-th component. The volume fraction, ϕ_i was calculated as

$$\phi_i = \frac{x_i v_i}{\sum_{i=1} x_i v_i}. \tag{31}$$

The values of all the derived parameters from density and ultrasonic velocity data are listed in Table 3. The values of molar volume (V), molar volume at absolute zero (V_0), actual volume of the molecules per mole (b), collision factor (S), surface area (Y), critical temperature (T_{c}) and the ratio of principle heat capacities (γ) for the pure components are listed in Table 4. The results of V^{E}, Δu, κ_s^{E}, L_{f}^{E}, r^{E} and Z^{E} have been fitted to the Redlich–Kister equation [14] of the type

$$\Delta Y = x_1 x_2 \sum_{i=1}^{k} A_i (x_1 - x_2)^{i-1}, \tag{32}$$

where k is the number of estimated parameters and A_i, the polynomial coefficients were obtained by fitting the equation to the experimental results by least-squares regression method. The standard deviations σ, for V^{E}, Δu, κ_s^{E}, L_{f}^{E} and Z^{E} were calculated using the relation

$$\sigma(Y) = \left[\frac{\sum\left(y_{\exp t} - y_{\text{calc}}\right)^2}{N - n}\right]^{1/2}, \tag{33}$$

Table 3. Molar sound velocities (R_m), molecular radii (r), thermal expansivities (α), thermoacoustical parameters (K, K', K'', $\overline{V}$, C_1), available volumes (V_a), intermolecular free lengths (L_f) computed by different methods, acoustic impedances (Z) and excess functions L_f^E and Z^E.

x_1	u (m s^{-1})	$R_m \times 10^6$ (m^3 mol^{-1})·(ms^{-1})$^{1/3}$	r (Å)	α (kK^{-1})	K	K'	K''	$\overline{V}$ (m^3 mol^{-1})	C_1
Panel A: Chloroform (1) + Octan-1-ol (2) (298.15 K)									
0.0000	1348.29	1750.6	2.459	0.8501	3.8084	3.7071	−0.1013	1.2161	8.6167
0.0351	1336.53	1715.8	2.444	0.8860	3.7355	3.6904	−0.0451	1.2239	8.4710
0.1707	1290.65	1584.1	2.388	0.9318	3.6516	3.6716	0.0200	1.2336	8.3032
0.2493	1262.42	1508.0	2.353	0.9443	3.6304	3.6669	0.0365	1.2362	8.2607
0.2913	1246.90	1467.6	2.335	0.9679	3.5917	3.6584	0.0668	1.2411	8.1833
0.3610	1220.18	1400.3	2.303	0.9776	3.5764	3.6551	0.0787	1.2431	8.1528
0.3986	1205.49	1364.0	2.285	0.9874	3.5613	3.6519	0.0906	1.2451	8.1226
0.5134	1160.33	1254.1	2.230	1.0390	3.4872	3.6363	0.1490	1.2556	7.9745
0.6148	1119.27	1157.6	2.178	1.0794	3.4349	3.6256	0.1907	1.2638	7.8697
0.6369	1110.30	1136.8	2.166	1.0899	3.4220	3.6230	0.2010	1.2659	7.8440
0.6616	1100.31	1113.5	2.153	1.1000	3.4099	3.6206	0.2107	1.2679	7.8197
0.7463	1066.55	1034.5	2.107	1.1160	3.3912	3.6169	0.2257	1.2710	7.7825
0.8015	1045.09	983.6	2.075	1.1132	3.3944	3.6175	0.2231	1.2705	7.7889
0.9017	1009.80	892.8	2.014	1.2263	3.2779	3.5959	0.3180	1.2923	7.5559
0.9822	987.94	822.1	1.963	1.2828	3.2290	3.5877	0.3588	1.3029	7.4579
1.0000	983.80	806.4	1.950	1.2974	3.2171	3.5858	0.3687	1.3057	7.4342

x_1	$V_a \times 10^6$ (Thermodynamic) (m^3 mol^{-1})	$V_a \times 10^6$ (Ultrasonic) (m^3 mol^{-1})	$V_a \times 10^6$ (TAP) (m^3 mol^{-1})	L_f (Thermodynamic) (Å)	L_f (Ultrasonic) (Å)	L_f (TAP) (Å)	L_f^E (Å)	$Z \times 10^{-3}$ (kg m^{-2} s^{-1})	$Z^E \times 10^{-3}$ (kg m^{-2} s^{-1})
0.0000	26.52	24.93	33.66	0.5011	0.4710	0.6360	0.0000	1108.05	0.00
0.0351	26.28	25.65	33.21	0.5033	0.4912	0.6357	0.0009	1114.14	−5.88
0.1707	25.32	28.13	31.14	0.5120	0.5689	0.6298	0.0045	1138.82	−27.35
0.2493	24.73	29.44	29.90	0.5170	0.6153	0.6249	0.0065	1153.78	−39.17
0.2913	24.41	30.09	29.27	0.5196	0.6404	0.6229	0.0076	1161.99	−45.25
0.3610	23.86	31.11	28.15	0.5237	0.6827	0.6178	0.0091	1176.11	−54.88
0.3986	23.56	31.60	27.55	0.5258	0.7054	0.6150	0.0098	1184.20	−59.58
0.5134	22.57	32.79	25.74	0.5317	0.7725	0.6063	0.0113	1212.02	−70.84

0.6148	21.65	33.50	24.10	0.5361	0.8295	0.5968	0.0119	1240.38	−77.03
0.6369	21.44	33.60	23.75	0.5369	0.8414	0.5946	0.0119	1247.23	−77.70
0.6616	21.20	33.69	23.34	0.5378	0.8543	0.5920	0.0118	1255.25	−78.08
0.7463	20.36	33.76	21.93	0.5401	0.8954	0.5817	0.0110	1286.50	−75.70
0.8015	19.79	33.62	20.99	0.5411	0.9191	0.5739	0.0099	1310.42	−70.58
0.9017	18.69	32.83	19.36	0.5412	0.9506	0.5607	0.0062	1366.74	−48.35
0.9822	17.75	31.58	17.99	0.5396	0.9601	0.5471	0.0015	1431.04	−11.48
1.0000	17.52	31.22	17.68	0.5387	0.9600	0.5436	0.0000	1448.58	0.00

x_1	u (m s^{-1})	$R_m \times 10^6$ (m^3 mol^{-1})$\cdot$(ms^{-1}) $^{1/3}$	r (Å)	α (kK^{-1})	K	K'	K''	$\overline{V}$ (m^3 mol^{-1})	C_1
Panel B: 1,2-Dichloroethane (1) + Octan-1-ol (2) (298.15 K)									
0.0000	1348.29	1750.6	2.459	0.8501	3.8084	3.7071	−0.1013	1.2161	8.617
0.0492	1338.36	1704.6	2.439	0.8658	3.7758	3.6996	−0.0762	1.2195	8.552
0.0906	1328.66	1665.1	2.421	0.8933	3.7215	3.6872	−0.0343	1.2254	8.443
0.2242	1301.89	1541.2	2.363	0.9545	3.6134	3.6632	0.0498	1.2383	8.227
0.3387	1277.56	1435.7	2.311	1.0094	3.5287	3.6449	0.1163	1.2496	8.057
0.4467	1255.47	1337.8	2.261	1.0464	3.4773	3.6342	0.1569	1.2571	7.955
0.4963	1245.89	1293.7	2.237	1.0449	3.4793	3.6346	0.1553	1.2568	7.959
0.5965	1228.15	1205.7	2.187	0.9971	3.5468	3.6488	0.1020	1.2471	8.094
0.6663	1216.1	1143.6	2.150	1.0116	3.5255	3.6442	0.1188	1.2501	8.051
0.7304	1206.47	1086.8	2.115	1.0272	3.5034	3.6396	0.1362	1.2533	8.007
0.7590	1202.08	1060.9	2.098	1.0659	3.4519	3.6290	0.1771	1.2611	7.904
0.9085	1189.44	924.7	2.005	1.1815	3.3209	3.6036	0.2828	1.2838	7.642
0.9535	1191.69	1750.6	1.975	1.1858	3.3166	3.6028	0.2863	1.2846	7.633
0.9616	1192.66	1704.6	1.968	1.2067	3.2962	3.5992	0.3029	1.2886	7.592
0.9896	1193.92	1665.1	1.949	1.1747	3.3278	3.6049	0.2771	1.2825	7.656
1.0000	1194.06	1541.2	1.942	1.1824	3.3200	3.6035	0.2834	1.2839	7.640

x_1	$V_a \times 10^6$ (Thermodynamic) m^3 mol^{-1})	$V_a \times 10^6$ (Ultrasonic) (m^3 mol^{-1})	$V_a \times 10^6$ (TAP) (m^3 mol^{-1})	L_f (Thermodynamic) (Å)	L_f (Ultrasonic) (Å)	L_f (TAP) (Å)	L_{sf}^E (Å)	$Z \times 10^{-3}$ (kg m^{-2} s^{-1})	$Z^E \times 10^{-3}$ (kg m^{-2} s^{-1})
0.0000	26.52	24.93	33.66	0.5011	0.4710	0.6360	0.0000	1108.05	0.00
0.0492	26.21	25.29	32.91	0.5051	0.4874	0.6342	0.0012	1113.49	−13.20

(*continued*)

Table 3. Continued.

x_1	$V_a \times 10^6$ (Thermodynamic) $\mathrm{m^3\,mol^{-1}}$)	$V_a \times 10^6$ (Ultrasonic) ($\mathrm{m^3\,mol^{-1}}$)	$V_a \times 10^6$ (TAP) ($\mathrm{m^3\,mol^{-1}}$)	L_f (Thermodynamic) (Å)	L_f (Ultrasonic) (Å)	L_f (TAP) (Å)	L_f^E (Å)	$Z \times 10^{-3}$ ($\mathrm{kg\,m^{-2}\,s^{-1}}$)	$Z^E \times 10^{-3}$ ($\mathrm{kg\,m^{-2}\,s^{-1}}$)
0.0906	25.94	25.69	32.31	0.5083	0.5034	0.6333	0.0021	1117.57	−24.81
0.2242	25.02	26.30	30.27	0.5190	0.5455	0.6278	0.0053	1136.50	−56.50
0.3387	24.19	26.66	28.49	0.5282	0.5822	0.6219	0.0080	1155.15	−81.23
0.4467	23.36	26.70	26.76	0.5367	0.6134	0.6147	0.0105	1177.00	−−100.30
0.4963	22.97	26.61	25.94	0.5407	0.6263	0.6106	0.0117	1188.69	−107.41
0.5965	22.15	26.17	24.22	0.5486	0.6480	0.5998	0.0140	1217.10	−116.97
0.6663	21.53	25.71	23.07	0.5532	0.6607	0.5929	0.0147	1241.65	−118.86
0.7304	20.92	25.11	22.00	0.5569	0.6685	0.5858	0.0147	1269.15	−115.65
0.7590	20.62	24.81	21.55	0.5580	0.6714	0.5832	0.0143	1283.07	−112.57
0.9085	18.93	22.39	18.96	0.5598	0.6623	0.5607	0.0076	1387.71	−64.57
0.9535	18.38	21.30	18.14	0.5592	0.6482	0.5518	0.0045	1433.44	−35.89
0.9616	18.25	21.05	17.98	0.5583	0.6439	0.5499	0.0031	1444.64	−27.76
0.9896	17.90	20.39	17.45	0.5576	0.6350	0.5434	0.0009	1475.54	−7.47
1.0000	17.77	20.16	17.26	0.5573	0.6323	0.5413	0.0000	1486.95	0.00

x_1	u ($\mathrm{m\,s^{-1}}$)	$R_m \times 10^6$ ($\mathrm{m^3\,mol^{-1}}$)$\cdot$($\mathrm{ms^{-1}}$) $^{1/3}$	r (Å)	α ($\mathrm{kK^{-1}}$)	K	K'	K''	$\overline{V}$ ($\mathrm{m^3\,mol^{-1}}$)	C_1
Panel C: 1,1,2,2-Tetrachloroethane (1) + Octan-1-ol (2) (298.15 K)									
0.0000	1348.29	1750.6	2.459	0.8501	3.8084	3.7071	−0.1013	1.2161	8.6167
0.0391	1337.38	1704.6	2.448	0.8581	3.7916	3.7032	−0.0884	1.2179	8.5833
0.0672	1329.69	1665.1	2.440	0.8649	3.7775	3.7000	−0.0775	1.2193	8.5551
0.1413	1309.54	1541.2	2.419	0.8770	3.7532	3.6944	−0.0588	1.2219	8.5064
0.2172	1288.88	1435.7	2.397	0.8885	3.7308	3.6893	−0.0415	1.2244	8.4616
0.2704	1274.92	1337.8	2.382	0.8950	3.7183	3.6865	−0.0318	1.2258	8.4366
0.4038	1241.29	1293.7	2.342	0.9147	3.6818	3.6783	−0.0035	1.2300	8.3637
0.4464	1231.12	1205.7	2.330	0.9146	3.6820	3.6784	−0.0037	1.2299	8.3641
0.5512	1208.1	1143.6	2.297	0.9259	3.6619	3.6739	0.0120	1.2323	8.3238
0.6371	1190.86	1086.8	2.270	0.9456	3.6280	3.6664	0.0383	1.2365	8.2561
0.6830	1182.63	1060.9	2.255	0.9517	3.6180	3.6642	0.0462	1.2377	8.2360

0.7481	1172.37	924.7	2.233	0.9603	3.6039	3.6611	0.0572	1.2395	8.2077
0.8561	1158.78	885.0	2.196	0.9804	3.5720	3.6542	0.0822	1.2437	8.1440
0.9321	1153.22	876.9	2.170	0.9650	3.5964	3.6595	0.0631	1.2405	8.1927
0.9834	1150.51	852.2	2.151	0.9819	3.5698	3.6537	0.0839	1.2440	8.1397
1.0000	1149.63	843.1	2.144	0.9844	3.5659	3.6529	0.0870	1.2445	8.1318

x_1	$V_a \times 10^6$ (Thermodynamic) ($m^3 mol^{-1}$)	$V_a \times 10^6$ (Ultrasonic) ($m^3 mol^{-1}$)	$V_a \times 10^6$ (TAP) ($m^3 mol^{-1}$)	L_f (Thermodynamic) (Å)	L_f (Ultrasonic) (Å)	L_f (TAP) (Å)	L_f^E (Å)	$Z \times 10^{-3}$ ($kg\,m^{-2}\,s^{-1}$)	$Z^E \times 10^{-3}$ ($kg\,m^{-2}\,s^{-1}$)
0.0000	26.52	24.93	33.66	0.5011	0.4710	0.6360	0.0000	1108.05	0.00
0.0391	26.16	25.67	33.25	0.4987	0.4894	0.6339	0.0004	1126.40	−9.72
0.0672	25.89	26.16	32.95	0.4970	0.5023	0.6325	0.0008	1139.82	−16.52
0.1413	25.21	27.41	32.16	0.4927	0.5356	0.6285	0.0017	1175.59	−33.92
0.2172	24.52	28.59	31.36	0.4882	0.5693	0.6243	0.0027	1213.07	−50.94
0.2704	24.04	29.31	30.78	0.4850	0.5914	0.6211	0.0032	1240.72	−61.54
0.4038	22.83	30.78	29.35	0.4765	0.6426	0.6127	0.0043	1314.54	−83.48
0.4464	22.44	31.14	28.88	0.4737	0.6574	0.6095	0.0045	1339.87	−88.74
0.5512	21.50	31.75	27.73	0.4666	0.6891	0.6019	0.0049	1407.19	−96.75
0.6371	20.72	31.99	26.81	0.4604	0.7108	0.5957	0.0048	1467.86	−97.76
0.6830	20.30	32.00	26.30	0.4569	0.7203	0.5920	0.0047	1503.01	−95.52
0.7481	19.71	31.87	25.58	0.4519	0.7306	0.5865	0.0043	1557.03	−88.28
0.8561	18.73	31.29	24.38	0.4429	0.7402	0.5767	0.0030	1658.68	−64.20
0.9321	18.03	30.55	23.48	0.4362	0.7391	0.5680	0.0018	1742.45	−35.02
0.9834	17.55	29.94	22.90	0.4313	0.7358	0.5628	0.0005	1805.12	−9.17
1.0000	17.39	29.74	22.71	0.4296	0.7346	0.5609	0.0000	1826.23	0.00

x_1	u ($m\,s^{-1}$)	$R_m \times 10^6$ ($m^3 mol^{-1}$) $\cdot(ms^{-1})^{1/3}$	r (Å)	α (kK^{-1})	K	K'	K''	$\overline{V}$ ($m^3 mol^{-1}$)	C_1
Panel D: Chloroform (1) + Octan-1-ol (2) (308.15 K)									
0.0000	1314.45	1750.7	2.464	0.8574	3.7353	3.6903	−0.0449	1.2239	8.4705
0.0351	1302.96	1716.5	2.450	0.8940	3.6654	3.6746	0.0093	1.2319	8.3308
0.1707	1256.00	1584.5	2.393	0.9406	3.5850	3.6570	0.0720	1.2420	8.1700

(*continued*)

Table 3. Continued.

x_1	u (m s^{-1})	$R_m \times 10^6$ (m^3 mol^{-1})·(ms^{-1})$^{1/3}$	r (Å)	α (kK^{-1})	K	K'	K''	$\overline{V}$ (m^3 mol^{-1})	C_1
0.2493	1227.78	1508.3	2.359	0.9533	3.5646	3.6526	0.0880	1.2447	8.1293
0.2913	1212.46	1468.2	2.341	0.9774	3.5276	3.6447	0.1171	1.2498	8.0552
0.3610	1186.27	1400.9	2.309	0.9873	3.5130	3.6416	0.1286	1.2519	8.0260
0.3986	1172.07	1364.8	2.291	0.9973	3.4985	3.6386	0.1401	1.2540	7.9971
0.5134	1127.14	1255.0	2.236	1.0499	3.4278	3.6241	0.1964	1.2649	7.8556
0.6148	1086.71	1158.8	2.184	1.0912	3.3778	3.6143	0.2365	1.2733	7.7557
0.6369	1077.32	1137.8	2.172	1.1019	3.3656	3.6120	0.2464	1.2755	7.7311
0.6616	1067.11	1114.5	2.159	1.1122	3.3540	3.6098	0.2558	1.2776	7.7080
0.7463	1033.75	1035.3	2.113	1.1286	3.3363	3.6065	0.2702	1.2809	7.6725
0.8015	1012.85	984.3	2.081	1.1257	3.3393	3.6070	0.2677	1.2803	7.6786
0.9017	977.25	894.1	2.021	1.2415	3.2286	3.5877	0.3590	1.3030	7.4573
0.9822	953.61	823.1	1.969	1.2994	3.1823	3.5805	0.3982	1.3140	7.3646
1.0000	949.98	807.5	1.957	1.3145	3.1711	3.5789	0.4078	1.3169	7.3422

x_1	$V_a \times 10^6$ (Thermodynamic) (m^3 mol^{-1})	$V_a \times 10^6$ (Ultrasonic) (m^3 mol^{-1})	$V_a \times 10^6$ (TAP) (m^3 mol^{-1})	L_f (Thermodynamic) (Å)	L_f (Ultrasonic) (Å)	L_f (TAP) (Å)	L_f^E (Å)	$Z \times 10^{-3}$ (kg m^{-2} s^{-1})	$Z^E \times 10^{-3}$ (kg m^{-2} s^{-1})
0.0000	27.89	28.52	34.07	0.5269	0.5389	0.6438	0.0000	1071.06	0.000
0.0351	27.64	29.18	33.62	0.5294	0.5588	0.6439	0.0010	1076.53	−5.40
0.1707	26.66	31.57	31.54	0.5391	0.6386	0.6378	0.0047	1097.92	−25.98
0.2493	26.05	32.77	30.28	0.5445	0.6849	0.6328	0.0066	1111.52	−36.72
0.2913	25.72	33.35	29.64	0.5475	0.7098	0.6309	0.0077	1118.96	−42.27
0.3610	25.15	34.22	28.51	0.5520	0.7510	0.6257	0.0092	1132.25	−50.58
0.3986	24.83	34.62	27.91	0.5543	0.7728	0.6229	0.0098	1140.00	−54.45
0.5134	23.82	35.64	26.08	0.5610	0.8395	0.6143	0.0115	1165.12	−64.86
0.6148	22.86	36.16	24.43	0.5660	0.8953	0.6048	0.0120	1191.29	−70.09
0.6369	22.65	36.26	24.07	0.5670	0.9079	0.6026	0.0120	1196.99	−71.23
0.6616	22.40	36.32	23.66	0.5681	0.9211	0.6000	0.0120	1203.98	−71.88
0.7463	21.52	36.24	22.23	0.5708	0.9611	0.5895	0.0110	1233.02	−69.09
0.8015	20.92	35.97	21.28	0.5720	0.9833	0.5816	0.0097	1255.85	−63.34

0.9017	19.79	35.06	19.64	0.5730	1.0154	0.5686	0.0064	1306.47	−43.73
0.9822	18.81	33.78	18.26	0.5718	1.0270	0.5550	0.0016	1363.59	−11.54
1.0000	18.57	33.37	17.94	0.5710	1.0259	0.5515	0.0000	1380.64	0.00

x_1	u (m s^{-1})	$R_m \times 10^6$ (m^3 mol^{-1})·(ms^{-1})$^{1/3}$	r (Å)	α (kK^{-1})	K	K'	K''	$\overline{V}$ (m^3 mol^{-1})	C_1
Panel E: 1,2-Dichloroethane (1) + Octan-1-ol (2) (308.15 K)									
0.0000	1314.45	1750.7	2.465	0.8574	3.7353	3.6903	−0.0449	1.224	8.471
0.0492	1304.55	1704.9	2.444	0.8733	3.7040	3.6833	−0.0207	1.227	8.408
0.0906	1294.70	1665.6	2.427	0.9014	3.6519	3.6717	0.0197	1.234	8.304
0.2242	1267.67	1542.3	2.369	0.9637	3.5484	3.6491	0.1007	1.247	8.097
0.3387	1243.02	1437.2	2.317	1.0197	3.4674	3.6322	0.1648	1.259	7.935
0.4467	1220.75	1339.4	2.266	1.0575	3.4183	3.6223	0.2039	1.266	7.837
0.4963	1211.02	1295.1	2.242	1.0559	3.4202	3.6226	0.2024	1.266	7.840
0.5965	1192.00	1205.8	2.193	1.0071	3.4846	3.6357	0.1511	1.256	7.969
0.6663	1179.94	1143.8	2.156	1.0220	3.4644	3.6315	0.1672	1.259	7.929
0.7304	1171.12	1087.2	2.121	1.0379	3.4433	3.6273	0.1840	1.262	7.887
0.7590	1166.78	1061.7	2.104	1.0774	3.3940	3.6175	0.2235	1.271	7.788
0.9085	1154.10	926.4	2.010	1.1957	3.2693	3.5945	0.3252	1.294	7.539
0.9535	1154.90	886.4	1.980	1.2001	3.2652	3.5938	0.3285	1.295	7.530
0.9616	1155.40	878.3	1.974	1.2215	3.2459	3.5905	0.3446	1.299	7.492
0.9896	1155.87	853.1	1.955	1.1887	3.2759	3.5956	0.3197	1.293	7.552
1.0000	1155.85	844.0	1.948	1.1965	3.2685	3.5943	0.3258	1.294	7.537

x_1	$V_a \times 10^6$ (Thermodynamic) (m^3 mol^{-1})	$V_a \times 10^6$ (Ultrasonic) (m^3 mol^{-1})	$V_a \times 10^6$ (TAP) (m^3 mol^{-1})	L_f (Thermodynamic) (Å)	L_f (Ultrasonic) (Å)	L_f (TAP) (Å)	L_f^E (Å)	$Z \times 10^{-3}$ (kg m^{-2} s^{-1})	$Z^E \times 10^{-3}$ (kg m^{-2} s^{-1})
0.0000	27.89	28.52	34.07	0.5269	0.5389	0.6438	0.0000	1071.06	0.00
0.0492	27.57	28.81	33.32	0.5313	0.5552	0.6420	0.0012	1075.96	−12.38
0.0906	27.29	29.16	32.71	0.5349	0.5716	0.6412	0.0022	1079.28	−23.61
0.2242	26.36	29.60	30.65	0.5468	0.6141	0.6359	0.0055	1096.06	−53.76
0.3387	25.51	29.82	28.86	0.5570	0.6513	0.6302	0.0083	1112.58	−77.46
0.4467	24.65	29.70	27.11	0.5666	0.6827	0.6231	0.0109	1132.48	−95.50

(continued)

Table 3. Continued.

x_1	$V_a \times 10^6$ (Thermodynamic) ($m^3 mol^{-1}$)	$V_a \times 10^6$ (Ultrasonic) ($m^3 mol^{-1}$)	$V_a \times 10^6$ (TAP) ($m^3 mol^{-1}$)	L_f (Thermodynamic) (Å)	L_f (Ultrasonic) (Å)	L_f (TAP) (Å)	L_f^E (Å)	$Z \times 10^{-3}$ ($kg m^{-2} s^{-1}$)	$Z^E \times 10^{-3}$ ($kg m^{-2} s^{-1}$)
0.4963	24.25	29.54	26.28	0.5709	0.6955	0.6189	0.0121	1143.35	−102.06
0.5965	23.38	29.00	24.53	0.5793	0.7186	0.6079	0.0140	1169.49	−111.11
0.6663	22.73	28.42	23.37	0.5844	0.7308	0.6010	0.0147	1192.54	−112.58
0.7304	22.09	27.65	22.29	0.5886	0.7366	0.5939	0.0148	1219.31	−108.34
0.7590	21.80	27.31	21.84	0.5902	0.7394	0.5914	0.0145	1232.11	−105.58
0.9085	20.04	24.61	19.22	0.5934	0.7286	0.5691	0.0080	1330.57	−59.63
0.9535	19.47	23.50	18.39	0.5929	0.7158	0.5602	0.0047	1372.71	−33.30
0.9616	19.34	23.26	18.23	0.5922	0.7121	0.5583	0.0034	1382.62	−26.24
0.9896	18.97	22.56	17.69	0.5914	0.7036	0.5516	0.0008	1411.74	−6.96
1.0000	18.83	22.32	17.50	0.5912	0.7009	0.5496	0.0000	1422.35	0.00
x_1	u ($m s^{-1}$)	$R_m \times 10^6$ ($m^3 mol^{-1}$) · (ms^{-1}) $^{1/3}$	r (Å)	α (kK^{-1})	K	K'	K''	$\overline{V}$ ($m^3 mol^{-1}$)	C_1
Panel F: 1,1,2,2-Tetrachloroethane (1) + Octan-1-ol (2) (308.15 K)									
0.0000	1314.45	1750.7	2.464	0.8574	3.7353	3.6903	−0.0449	1.2239	8.4705
0.0391	1303.85	1723.0	2.453	0.8655	3.7192	3.6867	−0.0325	1.2257	8.4385
0.0672	1296.23	1703.4	2.445	0.8724	3.7057	3.6837	−0.0220	1.2272	8.4114
0.1413	1276.25	1652.3	2.424	0.8848	3.6823	3.6784	−0.0039	1.2299	8.3647
0.2172	1255.81	1600.7	2.403	0.8964	3.6609	3.6736	0.0127	1.2324	8.3218
0.2704	1242.04	1564.8	2.387	0.9031	3.6489	3.6710	0.0221	1.2339	8.2978
0.4038	1208.96	1476.3	2.348	0.9232	3.6140	3.6633	0.0493	1.2382	8.2279
0.4464	1199.12	1448.4	2.335	0.9231	3.6141	3.6633	0.0492	1.2382	8.2283
0.5512	1176.25	1380.9	2.302	0.9346	3.5949	3.6591	0.0643	1.2407	8.1897

0.6371	1159.45	1326.8	2.275	0.9547	3.5624	3.6521	0.0897	1.2450	8.1249
0.6830	1151.35	1298.2	2.260	0.9608	3.5528	3.6501	0.0973	1.2463	8.1056
0.7481	1141.27	1258.3	2.238	0.9696	3.5393	3.6472	0.1079	1.2481	8.0785
0.8561	1127.84	1192.9	2.201	0.9901	3.5088	3.6407	0.1319	1.2525	8.0176
0.9321	1121.96	1147.8	2.174	0.9744	3.5321	3.6457	0.1135	1.2491	8.0642
0.9834	1118.71	1117.4	2.155	0.9916	3.5067	3.6403	0.1336	1.2528	8.0134
1.0000	1117.78	1107.5	2.149	0.9942	3.5029	3.6395	0.1366	1.2533	8.0059

x_1	$V_a \times 10^6$ (Thermodynamic) ($m^3 mol^{-1}$)	$V_a \times 10^6$ (Ultrasonic) ($m^3 mol^{-1}$)	$V_a \times 10^6$ (TAP) ($m^3 mol^{-1}$)	L_f (Thermodynamic) (Å)	L_f (Ultrasonic) (Å)	L_f (TAP) (Å)	L_f^E (Å)	$Z \times 10^{-3}$ ($kg\,m^{-2}\,s^{-1}$)	$Z^E \times 10^{-3}$ ($kg\,m^{-2}\,s^{-1}$)
0.0000	27.89	28.52	34.07	0.5269	0.5389	0.6438	0.0000	1071.06	0.00
0.0391	27.50	29.19	33.65	0.5294	0.5566	0.6417	0.0005	1088.74	−9.18
0.0672	27.23	29.66	33.35	0.5391	0.5693	0.6403	0.0008	1101.52	−15.73
0.1413	26.52	30.82	32.56	0.5445	0.6023	0.6362	0.0019	1135.66	−32.47
0.2172	25.79	31.92	31.75	0.5475	0.6353	0.6319	0.0029	1171.45	−48.82
0.2704	25.29	32.57	31.17	0.5520	0.6570	0.6287	0.0035	1197.90	−58.96
0.4038	24.02	33.87	29.72	0.5543	0.7068	0.6201	0.0046	1268.59	−79.89
0.4464	23.61	34.16	29.24	0.5610	0.7207	0.6169	0.0048	1293.11	−84.64
0.5512	22.62	34.65	28.08	0.5660	0.7517	0.6092	0.0052	1357.41	−92.41
0.6371	21.80	34.77	27.15	0.5670	0.7723	0.6029	0.0052	1415.63	−93.20
0.6830	21.37	34.73	26.64	0.5681	0.7812	0.5991	0.0050	1449.33	−90.99
0.7481	20.75	34.52	25.91	0.5708	0.7908	0.5935	0.0046	1501.17	−83.90
0.8561	19.71	33.82	24.70	0.5720	0.7993	0.5836	0.0033	1598.57	−60.72
0.9321	18.98	33.00	23.78	0.5730	0.7978	0.5748	0.0018	1678.86	−32.65
0.9834	18.48	32.38	23.20	0.5718	0.7949	0.5694	0.0005	1737.99	−8.74
1.0000	18.31	32.16	23.00	0.5710	0.7936	0.5675	0.0000	1758.16	0.00

Table 4. Molar volumes (V), molar volumes at absolute zero (V_0), surface area factors (Y), collision factors (S), actual volumes (b) and ratio of molar heat capacities (γ).

System	T (K)	$V \times 10^6$ ($m^3\,mol^{-1}$)	$V_0 \times 10^6$ ($m^3\,mol^{-1}$)	$Y \times 10^{-4}$ ($m^3\,mol^{-1}$)	S	$b \times 10^6$ ($m^3\,mol^{-1}$)	γ	T_c
Octan-1-ol	298.15	158.463	131.939	1.059	3.558	37.527	1.165	652.45
	308.15	159.821	131.939	1.059	3.589	37.778	1.163	
Chloroform	298.15	81.075	63.555	0.651	2.541	18.724	1.495	536.50
	308.15	82.141	63.555	0.651	2.640	18.919	1.481	
1,2-Dichloroethane	298.15	79.467	61.696	0.638	3.210	18.473	1.453	523.15
	308.15	80.418	61.696	0.637	3.145	18.643	1.451	
1,1,2,2-Tetrachloroethane-octan-1-ol	298.15	105.663	88.268	0.810	4.109	24.883	1.387	661.15
	308.15	106.714	88.268	0.811	4.035	25.046	1.453	

where N is the number of data points and n is the number of coefficients. The calculated values of the polynomial coefficients A_1, A_2, A_3, A_4, A_5 and A_6 along with their standard deviation σ, are presented in Table 5. The curves presented in all the figures (Figures 1–7) are the calculated values and the points represent the experimental values.

The percentage deviations ($u\%$) were calculated using the relation

$$u\% = (u_{\mathrm{exp}} - u_{\mathrm{calc}}) \times 100/u_{\mathrm{exp}}, \tag{34}$$

where u_{exp} and u_{calc} are the experimental and calculated values of ultrasonic velocity, respectively.

The standard percentage deviations ($\sigma\%$) have also been calculated for each individual mixture, considering % deviations of ultrasonic velocity for all the mole fractions using the relation

$$\sigma\% = [\Sigma(u\%)^2/n - 1]^{½}, \tag{35}$$

where n represents the number of data points, i.e. 14. The predictive capability of each model in terms of an overall average percentage deviation (APD) and the standard percentage deviation ($\sigma\%$) is presented in Table 6.

For the systems under consideration, it has been observed that the mixing process does not proceed isochorically and is strongly influenced by intermolecular attractions connected with the volume effects due to structural changes. The intermolecular free length (L_f) computed using free length theory (FLT) increases with the increase in the mole fraction of chloroform and 1,2-DCE. The change in the slope of the isotherms of intermolecular free length as a function of mole fraction in the higher mole fraction region of chloroform and 1,2-DCE shows that the entropy effect related to the structural rearrangement of solvent molecules caused mainly by the disruption of the octan-1-ol multimers occurs in these two systems [31–33]. However, the mixing process is accompanied by the decrease in the intermolecular free length in the binary mixture of octan-1-ol + 1,1,2,2-TCE system on increasing the mole fraction of this haloalkane (Figure 1) indicating some specific type of intermolecular interactions in this system.

The variation of ultrasonic velocity (u) through a mixture depends on the increase or decrease in the values of intermolecular free length (L_f). In general, u and L_f vary in a reciprocal manner with the mole fraction of a mixture [34–36]. A perusal of the Table 3 reveals that the values of u, R_m and L_f vary inverse of each other with the composition for chloroform + octan-1-ol and 1,2-DCE + octan-1-ol systems. However, all these parameters decrease with the increase in the composition of mixture in the case of 1,1,2,2-TCE + octan-1-ol system indicating some specific type of intermolecular interactions in this system.

The plots of V^E with mole fraction x_1 for the binary mixtures of octan-1-ol with chloroform, 1,2-DCE and 1,1,2,2-TCE at 298.15 and 308.15 K are depicted in Figure 2. The V^E values are positive at both the temperatures for the 1,2-DCE + octan-1-ol [8,9,12] and chloroform + octan-1-ol binary [4] mixtures over the whole composition range; but for the binary mixture 1,1,2,2-TCE + octan-1-ol [10], the curve is sigmoidal and V^E is negative below $x_1 = 0.15$ and it becomes positive above this concentration range. A similar trend has been observed for these systems studied at different temperatures [8,9,12,4,10] and the maxima in V^E curves occur

Table 5. Coefficients of the Redlich–Kister equation and standard deviations for excess volume (V^E), ultrasonic velocity deviations (Δu), excess isentropic compressibilities (κ_s^E), excess intermolecular free lengths (L_f^E) and excess acoustic impedances (Z^E).

Property	T(K)	A_1	A_2	A_3	A_4	A_5	A_6	σ
				Chloroform(1) + Octan-1-ol(2)				
$V^E \times 10^6$ (m^3 mol^{-1})	298.15	2.425	0.572	−0.033	1.360	–	–	0.010
	308.15	2.625	0.708	−0.704	−0.941	1.460	2.1019	0.014
Δu (m s^{-1})	298.15	−2.067	−69.485	−37.980	−47.836	−26.453	26.5237	0.162
	308.15	0.673	−66.812	−49.378	3.661	−4.637	−39.2014	0.298
$\kappa_s^E \times 10^{12}$ (Pa^{-1})	298.15	28.566	59.230	38.911	59.392	22.729	−34.546	0.18
	308.15	31.899	66.734	50.666	−17.556	13.172	65.887	0.52
L_f^E (Å)	298.15	0.045	0.021	0.007	0.008	–	–	0.0001
	308.15	0.046	0.023	0.002	−0.006	0.012	0.0161	0.0001
$Z^E \times 10^{-3}$ (kg m^{-2} s^{-1})	298.15	−279.649	−171.862	−92.992	−85.597	−56.175	–	0.12
	308.15	−279.649	−171.862	−92.992	−85.597	−56.175	–	0.12
				1,2Dichloroethane(1) + Octan-1-ol(2)				
$V^E \times 10^6$ (m^3 mol^{-1})	298.15	3.956	5.396	3.634	−3.475	−4.147	–	0.029
	308.15	4.344	4.037	3.011	0.716	−2.881	−2.850	0.026
Δu (m s^{-1})	298.15	−102.693	−58.864	−43.665	−139.392	−9.270	132.475	0.817

	308.15	−99.792	−77.242	−31.697	–	–	–	0.585
$\kappa_s^E \times 10^{12}$ (Pa^{-1})	298.15	124.762	68.640	50.359	114.450	−33.462	151.952	0.84
	308.15	137.033	81.647	35.97	39.810	−35.511	−85.480	0.79
L_f^E (Å)	298.15	0.047	0.049	0.034	−0.012	−0.025	–	0.0002
	308.15	0.049	0.046	0.032	−0.005	−0.019	–	0.0002
$Z^E \times 10^{-3}$ (kg m^{-2} s^{-1})	298.15	−430.376	−241.570	−167.797	−176.271	32.037	165.130	1.12
	308.15	−409.830	−230.499	−139.997	−113.901	23.059	102.821	0.91
				1,1,2,2-Tetrachloroethane(1) + Octan-1-ol(2)				
$V^E \times 10^6$ (m^3 mol^{-1})	298.15	0.8996	1.0387	0.232	−0.0322	−0.4775	1.2331	0.006
	308.15	1.0013	0.9727	0.6254	0.5416	−0.9997	0.3839	0.004
Δu (m s^{-1})	298.15	−119.576	−43.6097	−14.622	−27.6775	17.5464	38.9366	0.140
	308.15	−115.92	−41.2555	−12.1356	−13.7426	21.1754	22.9423	0.116
$\kappa_s^E \times 10^{12}$ (Pa^{-1})	298.15	2.822	20.395	0.793	19.205	−19.380	−29.963	0.12
	308.15	4.892	20.808	0.942	9.900	−27.034	−20.164	0.12
L_f^E (Å)	298.15	0.019	0.0069	0.0011	−0.0038	0.0002	0.0087	0.0001
	308.15	0.0202	0.0068	0.0039	−0.0003	−0.0039	0.0039	0.0001
$Z^E \times 10^{-3}$ (kg m^{-2} s^{-1})	298.15	−374.747	−154.019	−61.4473	−46.873	21.6591	38.4256	0.15
	308.15	−357.808	−145.573	−59.7063	−37.7082	31.8513	33.8523	0.17

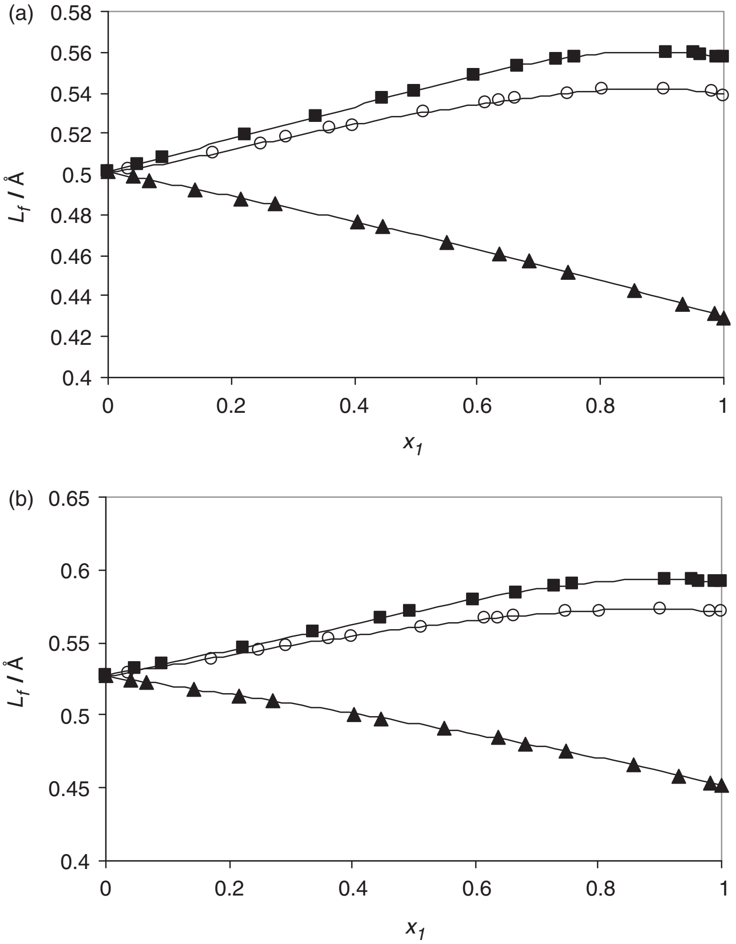

Figure 1. Intermolecular free lengths (L_f) *vs*. mole fraction (x_1) at (a) 298.15 and (b) 308.15 K, respectively for binary mixtures of octan-1-ol with (■) 1,2-dichloroethane, (○) chloroform and (▲) 1,1,2,2-tetrachloroethane.

around 0.6 in chloroform + octan-1-ol and around 0.7 in 1,2-DCE + octan-1-ol, and 1,1,2,2-TCE + octan-1-ol systems in the present investigations. The excess molar volume V^E decreases in the sequence: 1,2-DCE + octan-1-ol > chloroform + octan-1-ol > 1,1,2,2-TCE + octan-1-ol. An exactly similar type of behaviour has also been observed for the variation of V^E with mole fraction for the binary mixtures of 1,2-DCE + heptanol and 1,1,2,2-TCE + heptanol [1,6]. The magnitude of the maximum value of V^E increases slightly with the increase of temperature from 298.15 to 308.15 K.

The observed positive V^E values may be explained in terms of physical, chemical and structural factors [4,8,10,13,28,29,37–41]. The positive contribution might be due to the physical forces involving dispersive interactions between unlike molecules. The dispersive interactions are usually weak and the sign of V^E may be positive or negative. On the other hand, specific chemical interactions involving intermolecular H-bond formation, charge-transfer complex formation and the dipole–dipole

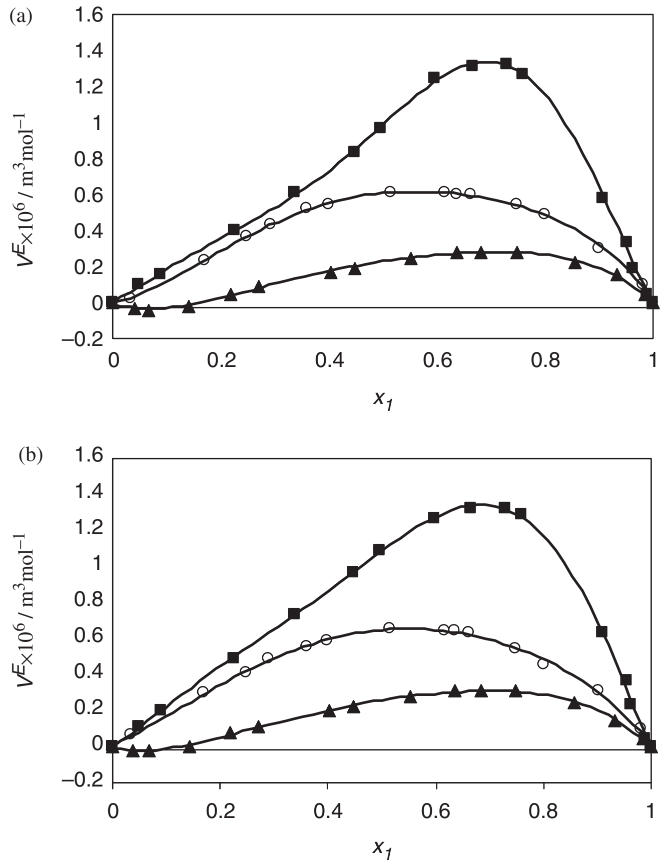

Figure 2. Excess molar volumes (V^E) *vs.* mole fraction (x_1) at (a) 298.15 and (b) 308.15 K, respectively for binary mixtures of octan-1-ol with (■) 1,2-dichloroethane, (○) chloroform and (▲) 1,1,2,2-tetrachloroethane.

interactions between various components of the mixture result in the decrease in volume. The variations in the associative equilibria of alkanol molecules might lead to all types of interactions. The sign and magnitude of V^E also varies with the structural characteristics of the components arising from the geometrical fitting of one component into the structure of the other component because of the differences in the size and shape of the components and the free volume. Since the molar volumes of octan-1-ol (158.46×10^{-6} and 159.82×10^{-6}) m^3 mole^{-1}, chloroform (81.08×10^{-6} and 82.14×10^{-6}) m^3 mole^{-1}, 1,2-DCE (79.47×10^{-6} and 80.42×10^{-6}) m^3 mole^{-1}, 1,1,2,2-TCE (105.66×10^{-6} and 106.71×10^{-6}) m^3 mole^{-1} at (298.15 and 308.15) K respectively differ considerably, it seems that the haloalkane molecules intercalate between the polymeric entities of octan-1-ol and disrupt their H-bonding [13]. Consequently, there is an increase in the total volume of solution. The destruction of short range orientation structural order present in pure liquids, namely, H-bonds in octan-1-ol and dipolar interaction in haloalkanes makes V^E positive since the aggregates have smaller volumes than the sum of their individual components [7] and the new possible H-bond interaction of the type Cl···H–O

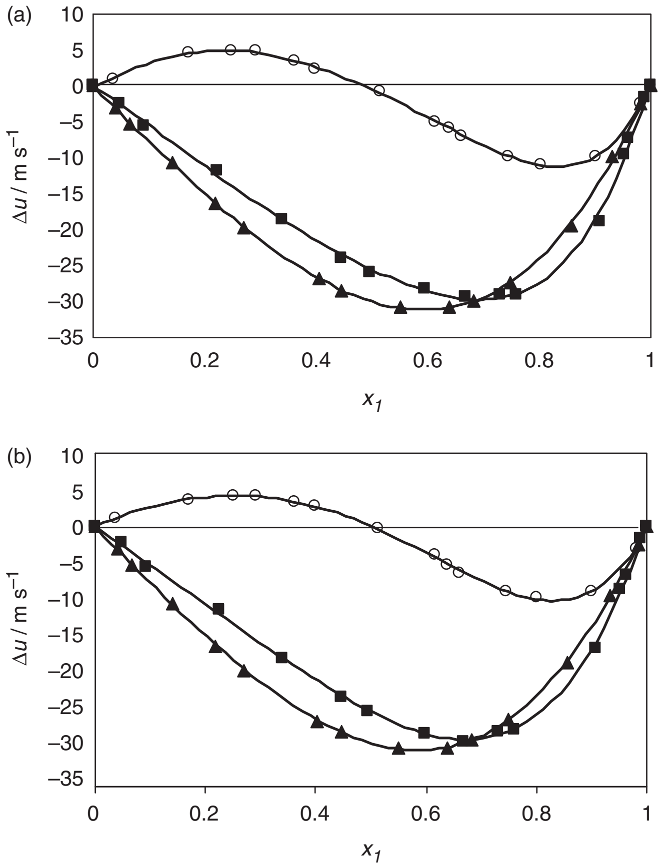

Figure 3. Deviations in ultrasonic velocities (Δu) *vs.* mole fraction (x_1) at (a) 298.15 and (b) 308.15 K, respectively for binary mixtures of octan-1-ol with (■) 1,2-dichloroethane, (○) chloroform and (▲) 1,1,2,2-tetrachloroethane.

between octan-1-ol and the haloalkane molecule is weaker than the dipolar interactions in pure haloalkanes and H-bonding in octan-1-ol. Since the structure-breaking effect and the effects of interaction between like and unlike molecules balance each other to different extents [8–11] in the 1,1,2,2-TCE and octan-1-ol mixtures, there is only a small increase in V^E values above $x_1 = 0.3$ in this case. At low concentration of 1,1,2,2-TCE, relatively stronger chemical interaction of the type Cl···H–O or charge transfer complex forming interaction is dominant resulting in the negative values of V^E, whereas at higher mole fractions of 1,1,2,2-TCE near $x_1 = 0.8$, weak dipole-dipole forces are dominant resulting in the positive values of V^E. At infinite dilution, structural rearrangement of the solvate structures occurs, dipole–dipole interactions become stronger and consequently V^E decreases. With the increase in the temperature, the interactions between unlike molecules become weaker and V^E increases. This trend can be correlated with the decrease in the population of octan-1-ol oligomers with increasing temperature meaning, thereby the rupture of the solvate structures occurs due to the increased Brownian motion [42] causing expansion of the molecular lattice.

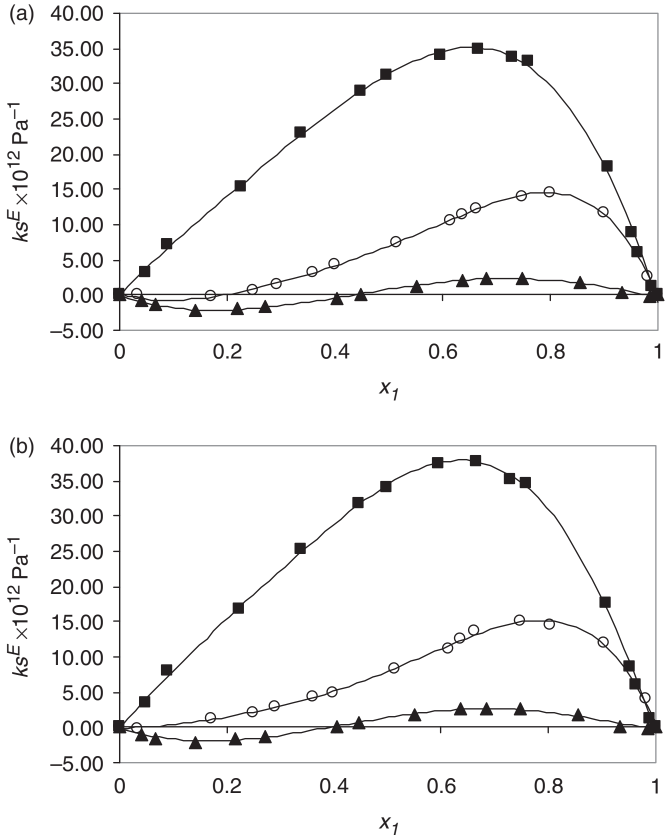

Figure 4. Excess isentropic compressibility (κ_S^{E}) *vs.* mole fraction (x_1) at (a) 298.15 and (b) 308.15 K, respectively for binary mixtures of octan-1-ol with (■) 1,2-dichloroethane, (○) chloroform and (▲) 1,1,2,2-tetrachloroethane.

For a system in which more than one type of interactions are involved between various components, the net result of contributions from different kinds of interactions is the deviation in the sound velocity of binary mixtures of the system. The Δu *versus* x_1 curves at 298.15 and 308.15 K are presented in Figure 3 and their variations are of quite different nature than those of the molar excess volumes (V^{E}). The Δu values for 1,2-DCE + octan-1-ol and 1,1,2,2-TCE + octan-1-ol are negative, and minima appear at about 0.7 and 0.6, respectively in these two cases at the two temperatures. For the case of chloroform + octan-1-ol mixture, a sigmoidal trend from positive to negative values is observed. In the low-concentration regions up to $x_1 \approx 0.5$, the Δu values are positive and in the higher concentration regions above $x_1 = 0.5$, the Δu values are negative. The absolute values of minima for all these mixtures decrease with the increase of temperature.

The results of κ_s^{E} *versus* x_1 at 298.15 and 308.15 K are presented in Figure 4. The κ_s^{E} values are positive over the entire composition range for 1,2-DCE + octan-1-ol and become more positive with the increase in temperature. Similar trend has been observed for this system studied at 303.15 K [8]. In the case of chloroform + octan-1-ol system, the κ_s^{E} values display small dip in the octan-1-ol-rich region and become

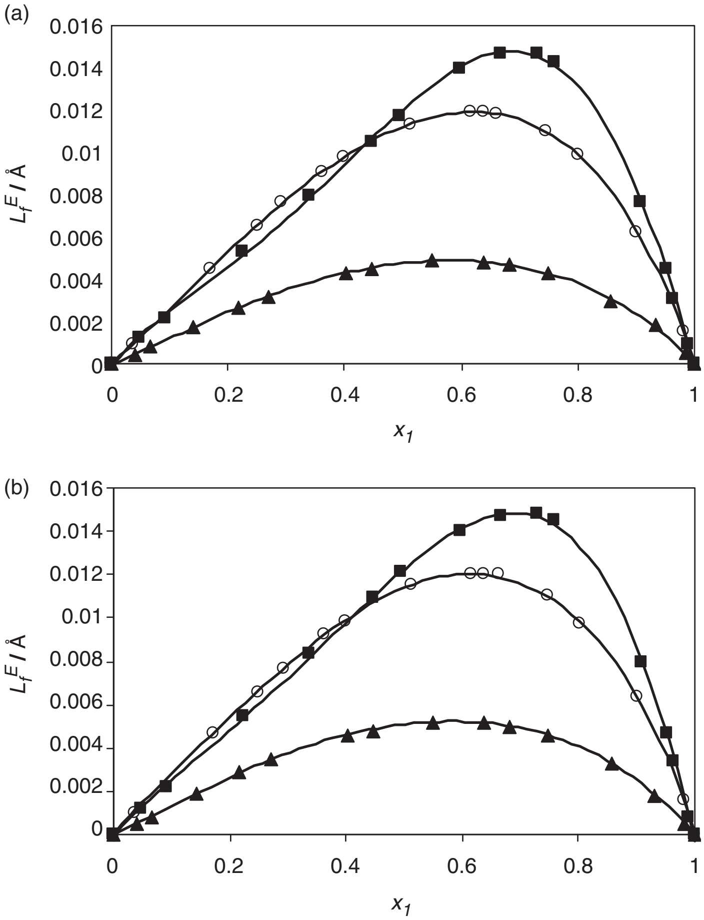

Figure 5. Excess intermolecular free lengths (L_f^E) *vs.* mole fraction (x_1) at (a) 298.15 and (b) 308.15 K, respectively for binary mixtures of octan-1-ol with (■) 1,2-dichloroethane, (○) chloroform and (▲)1,1,2,2-tetrachloroethane.

increasingly more positive with increase in the mole fraction of chloroform, and this behaviour is in close agreement with the trend observed for this system studied at 303.15 and 313.15 K [4]. In the case of 1,1,2,2-TCE + octan-1-ol system, the κ_s^E values are negative in the low-mole fraction region of 1,1,2,2-TCE up to $x_1 \approx 0.42$ and become more positive with increase in the mole fraction of 1,1,2,2-TCE. A similar trend has been observed for this system studied at 303.15 K [10]. These values decrease in the sequence: 1,2-DCE + octan-1-ol > chloroform + octan-1-ol > 1,1,2,2-TCE + octan-1-ol. This trend in the excess isentropic compressibility values correlates well with the intermolecular free length (L_f) and the volume changes connected with the structural rearrangement of the solvate structures in the higher mole fraction regions of the haloalkanes.

The intermolecular interaction strength of octan-1-ol and the haloalkanes may be related to the number of chlorine atoms present in the haloalkanes [13]. Due to the presence of four chlorine atoms in 1,1,2,2-TCE as compared to two in 1,2-DCE and

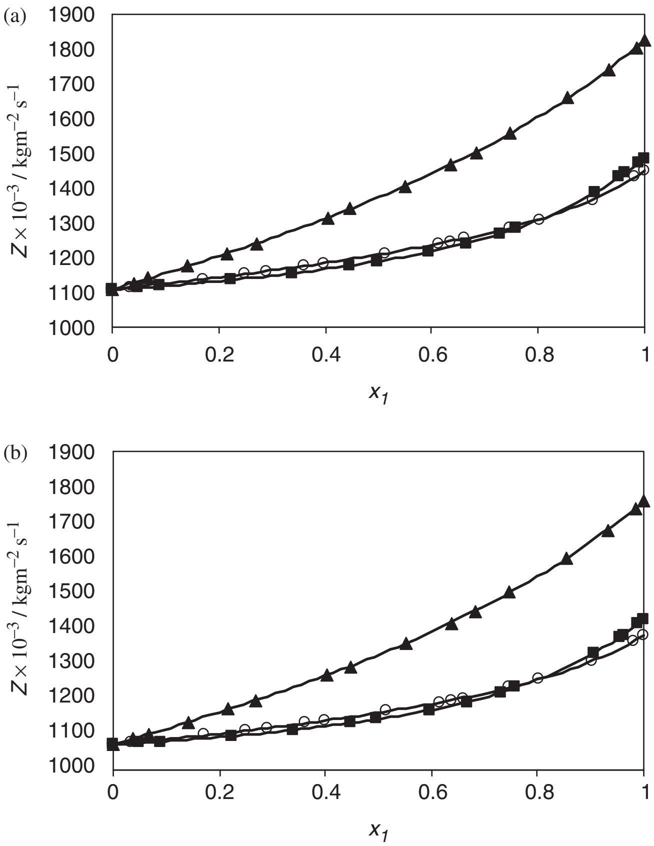

Figure 6. Acoustic impedances (Z) *vs.* mole fraction (x_1) at (a) 298.15 and (b) 308.15 K, respectively for binary mixtures of octan-1-ol with (■) 1,2-dichloroethane, (○) chloroform and (▲) 1,1,2,2-tetrachloroethane.

three in chloroform, four H-bonds of the type Cl $\cdots$ H–O will be formed between the OH group of octan-1-ol polymeric entities and 1,1,2,2-TCE molecule as compared to two and three Cl $\cdots$ H–O bonds in the 1,2-DCE and chloroform octan-1-ol system, respectively. The intermolecular interaction strength of the type Cl $\cdots$ H–O will vary in the order: 1,2-DCE + octan-1-ol < chloroform + octan-1-ol < 1,1,2,2-TCE + octan-1-ol. This observation is consistent with the trend observed for the V^E and κ_s^E data for these systems. The increase in the excess molar volume (V^E), negative deviation in sound velocity (Δu) and the positive excess isentropic compressibility (κ_s^E) support the main factor of gradual disruption of the self-associated octan-1-ol molecules and the weak physical intermolecular interactions [4,36,38,39] and the relatively weaker interactions of the type Cl $\cdots$ H–O between unlike molecules.

4. Theoretical analysis

The sound velocities have been calculated by different methods and the deviations between the experimental and calculated values for each mixture composition have

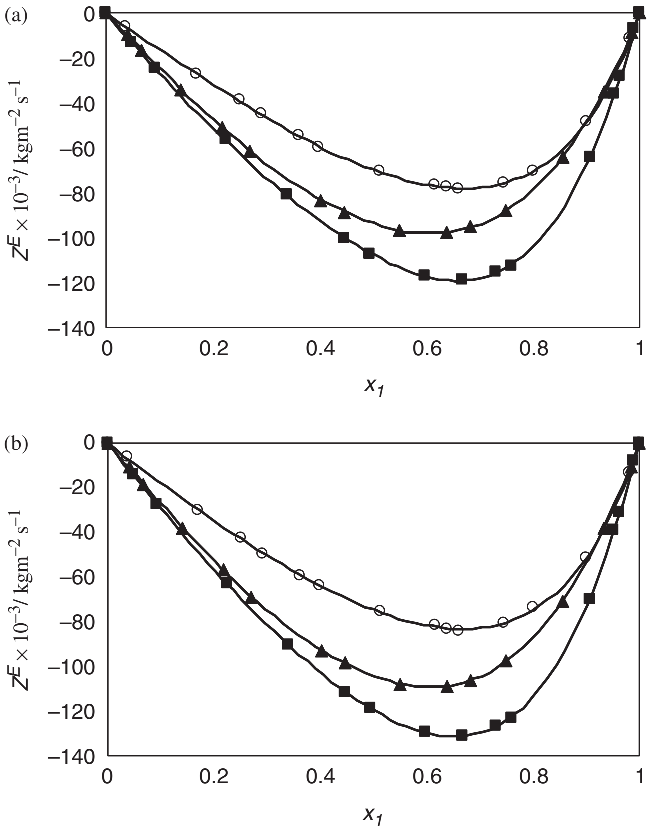

Figure 7. Excess acoustic impedances (Z^E) *vs.* mole fraction (x_1) at (a) 298.15 and (b) 308.15 K, respectively for binary mixtures of octan-1-ol with (■) 1,2-dichloroethane, (○) chloroform and (▲) 1,1,2,2-tetrachloroethane.

also been calculated. Other acoustical and thermoacoustical parameters necessary for computing intermolecular free lengths (L_f) have been calculated and are presented in Table 3. A close examination of Table 3 clearly illustrates fairly good agreement in the values of intermolecular free lengths computed from the thermodynamic, ultrasonic and thermoacoustic methods. The credibility of the results is further increased by the very small APD and standard percentage deviations (σ%) of ultrasonic velocities (Table 6) obtained using the Nomoto [21], Van Dael relation [22], Jacobson's FLT [23] and Schaaff's CFT [24–26] for all the systems under consideration. The σ% values will be discussed for the theoretical analysis of sound velocities for these systems.

The study of standard percentage deviations (σ%) presented in Table 6 reveals that the results of ultrasonic velocity for the chloroform + octan-1-ol system can be best explained by FLT formulations ($\sigma\% = 1.62$ and 1.69 at 298.15 and 308.15 K, respectively) followed by CFT formulations ($\sigma\% = 2.77$ and 1.71 at 298.15 and 308.15 K, respectively). For 1,2-DCE + octan-1-ol system, Van Dael relation gives minimum values of these deviations ($\sigma\% = 0.54$ and 0.53 at 298.15 and 308.15 K, respectively) followed by CFT formulations ($\sigma\% = 1.10$ and 1.07 at 298.15 and

Table 6. APD and standard percentage deviations (σ%) calculated by Nomoto (N), Van Dael (VD), FLT, CFT and TAP for chloroform-octan-1-ol, 1,2-dichloroethane-octan-1-ol and 1,1,2,2-tetrachloroethane-octan-1-ol systems.

		APD Values					σ % values				
System	T (K)	$(\mathrm{APD})_{\mathrm{N}}$	$(\mathrm{APD})_{\mathrm{VD}}$	$(\mathrm{APD})_{\mathrm{FLT}}$	$(\mathrm{APD})_{\mathrm{CFT}}$	$(\mathrm{APD})_{\mathrm{TAP}}$	$(\sigma\%)_{\mathrm{N}}$	(σ%) VD	(σ%) FLT	(σ%) CFT	(σ%) TAP
Chloroform-octan-1-ol	298.15	−2.92	2.47	0.89	2.49	−9.68	3.31	3.31	1.62	2.77	15.08
	308.15	−2.93	2.64	1.13	−1.61	−12.94	3.84	3.52	1.69	1.71	17.24
1,2-Dichloroethane-octan-1-ol	298.15	−2.27	−0.04	7.51	−0.93	−1.05	3.12	0.54	9.99	1.10	4.46
	308.15	−2.29	0.05	7.89	−0.89	−3.97	3.16	0.53	10.29	1.07	6.23
1,1,2,2-Tetrachloroethane-octan-1-ol	298.15	−2.11	−0.93	−1.79	− 4.05	−2.34	2.86	1.29	1.99	4.78	6.29
	308.15	−2.10	−0.92	0.15	− 4.02	−5.01	2.85	1.26	0.69	4.75	7.96

308.15 K, respectively). The results for the 1,1,2,2-TCE + octan-1-ol system can be satisfactorily explained by Van Dael relation ($\sigma\% = 1.29$ and 1.26) and FLT formulations ($\sigma\% = 1.99$ and 0.69) at 298.15 and 308.15 K, respectively. The thermoacoustical approach, in general, gives higher standard percentage deviations for all the binary mixtures.

Table 3 indicates that the values of intermolecular free lengths (L_f) for all the three binary mixtures obtained from the ultrasonic method are higher than the values computed from the thermodynamic and thermoacoustical method. This trend has also been observed for the binary liquid mixtures of 1,1,2,2-TCE with benzene, toluene, paraxylene, acetone, cyclohexane [43], liquid methane with liquid tetrafluoromethane [44] and the other multicomponent liquid mixtures [19]. It is evident from Table 3 that the L_f value for chloroform + octan-1-ol and 1,2-DCE + octan-1-ol systems increases with increase in the mole fraction and also increases with decrease in the ultrasonic velocity and vice versa. This relationship is not observed for the 1,1,2,2-TCE + octan-1-ol system in the Jacobson's FLT and for all the systems in the thermoacoustical approach (TAP), but it can be easily observed in all the three systems under study in the CFT formulations. The thermodynamic method [19] has been found to be better than the ultrasonic method for calculating the L_f values provided T is not very close to T_c because the right-hand side of Equation (10) vanishes when $T > T_c$. On the other hand, the ultrasonic method fails completely when the sound velocity of the liquid or their mixtures exceeds 1600 m s^{-1} since the right-hand side of Equation (13) disappears when $u > u_\infty$.

The available volume (V_a) computed using FLT and TAP decreases with the increase in mole fraction of haloalkanes for all the systems under consideration, but an opposite trend is observed for 1,1,2,2-TCE + octan-1-ol and chloroform + octan-1-ol systems in the case of Schaaffs CFT. The other parameters of the binary mixtures, actual volume of molecules per mole (b), collision factor (S), molecular radius (r) and acoustic impedance (Z), are also influenced by the disrupting of the structure of octan-1-ol on increasing the mole fraction of haloalkanes. The structure breaking effect and the variations of excess functions V^E, Δu, κ_s^E, L_f^E with mole fractions for these systems are consistent with the following order of molecular radii of haloalkanes (Table 3):

$$r_{\text{DCE}}(1.942\,\text{Å}) < r_{\text{CHCl}_3}(1.950\,\text{Å}) < r_{\text{TCE}}(2.144\,\text{Å}) \text{ at } 298.15\,\text{K}$$

$$r_{\text{DCE}}\ (1.948\,\text{Å}) < r_{\text{CHCl}_3}(1.957\,\text{Å}) < r_{\text{TCE}}(2.149\,\text{Å}) \text{ at } 308.15\,\text{K}.$$

The larger the molecular radius, greater is the structure breaking effect on the self-associated octan-1-ol, the smaller will be the values of the excess function L_f^E and the higher will be the strength of specific interactions between octan-1-ol and haloalkane molecule. The values of L_f^E obtained by the FLT method at the maximum of the curves (Figure 5) are in the order:

$$L^E_{\text{f, DCE−Oct}}\ (0.0147) > L^E_{\text{f, CHCl}_3\text{−Oct}}\ (0.0119) > L^E_{\text{f, TCE−Oct}}\ (0.0049) \text{ at } 298.15\,\text{K}$$

$$L^E_{\text{f, DCE−Oct}}\ (0.0148) > L^E_{\text{f, CHCl}_3\text{−Oct}}\ (0.0120) > L^E_{\text{f, TCE−Oct}}\ (0.0052) \text{ at } 308.15\,\text{K}.$$

The minimum values of L_f^E are consistent with the observation of minimum values of excess molar volume (V^E) and excess isentropic compressibility (κ_s^E) of the binary mixtures of 1,1,2,2-TCE + octan-1-ol system due to specific intermolecular interactions resulting in the formation of molecular complexes. The increase of Z with mole fraction of haloalkanes (Figure 6) suggests that weak physical interactions between unlike molecules dominate over the structure-breaking effect of octan-1-ol on the addition of haloalkanes [45]. The Z^E values at the minimum of the curves (Figure 7) are in the order:

$$Z^E_{\mathrm{DCE-Oct}}\ (-118.86) > Z^E_{\mathrm{TCE-Oct}}\ (-97.76) > Z^E_{\mathrm{CHCl_3-Oct}}\ (-78.08)\ \text{at}\ 298.15\,\mathrm{K}$$

$$Z^E_{\mathrm{DCE-Oct}}\ (-112.58) > Z^E_{\mathrm{TCE-Oct}}\ (-93.20) > Z^E_{\mathrm{CHCl_3-Oct}}\ (-71.88)\ \text{at}\ 308.15\,\mathrm{K}.$$

The excess acoustic impedance (Z^E) values are negative over the entire composition range for all the systems under consideration and become less negative with increasing temperature for all these mixtures. The negative deviations in Z^E values imply weak interactions between the component molecules [28,45,46]. The data for the higher negative values of Z^E for the 1,2-DCE + octan-1-ol system as compared to 1,1,2,2-TCE + octan-1-ol and chloroform + octan-1-ol systems in conjunction with the data of positive excess values V^E and κ_s^E support the observation of dominating effect of weak physical intermolecular interactions over the structure-breaking effect of the octan-1-ol on the addition of the haloalkanes.

5. Conclusion

The association interactions between the octan-1-ol molecules decrease with the increasing concentration of haloalkanes. Weak physical intermolecular interactions dominate over the structure breaking effect of octan-1-ol on the addition of haloalkanes. In the higher mole fraction regions of haloalkanes, a reduction of self-association and structural rearrangement of the solvate structures occurs due to solvation processes.

Acknowledgements

The authors are grateful to the Kurukshetra University authorities for providing the necessary facilities to carry out the research work.

References

[1] H. Houkhani and B. Samiety, J. Chem. Eng. Data **50**, 1911 (2005).

[2] M. Hasan, U.B. Kadam, A.P. Hiray, and A.B. Sawant, J. Chem.Eng. Data **51**, 60 (2006).

[3] M. Hasan, U.B. Kadam, A.P. Hiray, and A.B. Sawant, J. Chem. Eng. Data **51**, 671 (2006).

[4] M. Hasan, U.B. Kadam, A.P. Hiray, and A.B. Sawant, J. Chem. Eng. Data **51**, 1797 (2006).

[5] P.S. Nikem, L.N. Shirsat, and M.Hasan, J. Chem. Eng. Data **43**, 732 (1998).

[6] H. Houkhani and B. Samiety, Phys. Chem. Liq. **45** (5), 571 (2007).

[7] R.D. Peralta, R. Infante, G. Cortez, and A. Cisneros, Chem. Eng. Comm. **192**, 684 (2005).

[8] N.V. Choudary and P.R. Naidu, Can. J. Chem. **59** (14), 2210 (1981).

[9] N.V. Choudary and P.R. Naidu, Chem. Scripta **19** (2), 89 (1982).
[10] N.V. Choudary, A. Krishnaiah, and P.R. Naidu, J. Chem. Eng. Data **27** (4), 412 (1982).
[11] N.V. Choudary, J.C. Mouli, and P.R. Naidu, Acoust. Lett. **6** (4), 56 (1982).
[12] J.A. Salas and M. Katz, Fluid Phase Equilibr. **146** (1,2), 197 (1998).
[13] S.C. Bhatia, R. Bhatia, and G.P. Dubey, J. Mol. Liq. **144** (3), 163 (2009).
[14] O. Redlich and A.T. Kister, Ind. Eng. Chem. **40**, 345 (1948).
[15] A.S. Al-Jimaj, J.A. Al-Kandery, and A.M. Abdul-Latif, J. Chem. Eng. Data **52** (1), 216 (2007).
[16] M. Dzida, J. Chem. Eng. Data **52**, 521 (2007).
[17] T.M. Aminabhavi and V.B. Patil, J. Chem. Eng. Data **43**, 497 (1998).
[18] J. Nath, Fluid Phase Equilibr. **11**, 261 (2002).
[19] J.D. Pandey, R. Dey, and J. Chhabra, Phys Chem Comm. **6**, 55 (2003).
[20] J.A. Riddick, W.B. Bunger, and T.K. Sakano, *Organic Solvents, Physical Properties and Methods of Purification*, 4th ed. (Wiley Interscience, New York, 1986), Vol. 2.
[21] O. Nomoto, J. Phys. Soc. Jpn. **13**, 1528 (1958).
[22] W. Van Dael, *Thermodynamic Properties and Velocity of Sound* (Butterworth, London, 1975).
[23] B. Jacobson, Acta Chem. Scand. A **6**, 1485 (1952).
[24] W. Schaaffs, Acoustica **33**, 272 (1975).
[25] W. Schaaffs, *Molekularakustik* (Springer-Verlag, Berlin, 1963).
[26] R. Nutsch-Kuhnkies, Acoustica **15**, 383 (1965).
[27] A. Ali, A.K. Nain, D. Chand, and R. Ahmed, Phys. Chem. Liq. **43** (2), 205 (2005).
[28] A. Ali, K. Tewari, A.K. Nain, and V. Chakravortty, Phys. Chem. Liq. **38**, 459 (2000).
[29] G.C. Benson and O. Kiyohara, J. Chem. Thermodyn. **11**, 1061 (1979).
[30] W.E. Acree Jr, Phys. Chem. Liq. **16**, 113 (1986).
[31] R.J. Fort and W.R. Moore, Trans. Faraday Soc. **61**, 2102 (1965).
[32] H.T. French, J. Sol. Chem. **12** (12), 869 (1983).
[33] R.H. Stokes, J. Chem. Soc., Faraday Trans. **1** (73), 1140 (1977).
[34] A. Ali, A.K Nain, and M. Kamil, Thermochim. Acta **274**, 209 (1996).
[35] A. Ali, S. Hyder, and A.K. Nain, J.Mol. Liq. **79**, 89 (1999).
[36] A. Ali and A.K. Nain, Pramana-J. Phys. **58** (4), 695 (2002).
[37] H. Houkhani and K. Khanlarzadeh, J. Chem. Eng. Data **51**, 1226 (2006).
[38] C. Yang, H. Lai, Z. Liu, and P. Ma, J. Chem. Eng. Data **51**, 1345 (2006).
[39] T.M. Aminabhavi and K. Banerjee, J. Chem. Eng. Data **43**, 509 (1998).
[40] B. Giner, I. Gascon, A. Villares, P. Cea, and C. Lafuente, J. Chem. Eng. Data **51**, 1321 (2006).
[41] O. Kiyohara and G.C. Bensen, J. Chem. Thermodyn. **11**, 861 (1979).
[42] K. Bebek, G. Filosek, and S. Earnst, Mol. Quant. Acoust. **25**, 23 (2004).
[43] J.D. Pandey, G.P. Dubey, B.P. Shukla, and S.N. Dubey, J. Phy. **37** (6), 497 (1991).
[44] J.D. Pandey and S.N. Srivastav, Acustica **51**, 66 (1982).
[45] M. Das and M.N. Roy, J. Chem. Eng. Data **51**, 2225, 509 (2006).
[46] B. Gurung and M. Roy, J. Sol. Chem. **35** (12), 1587 (2006).